

# Testing, simulation and design of back-to-back built-up cold-formed steel unequal angle sections under axial compression

G. Beulah Gnana Ananthi<sup>1a</sup>, Krishanu Roy<sup>\*2</sup>, Boshan Chen<sup>2b</sup> and James B.P. Lim<sup>2c</sup>

<sup>1</sup> Division of Structural Engineering, College of Engineering Guindy Campus, Anna University, Chennai, India

<sup>2</sup> Department of Civil and Environmental Engineering, The University of Auckland, Auckland, New Zealand

(Received July 13, 2019, Revised November 7, 2019, Accepted November 9, 2019)

**Abstract.** In cold-formed steel (CFS) structures, such as trusses, transmission towers and portal frames, the use of back-to-back built-up CFS unequal angle sections are becoming increasingly popular. In such an arrangement, intermediate welds or screw fasteners are required at discrete points along the length, preventing the angle sections from buckling independently. Limited research is available in the literature on axial strength of back-to-back built-up CFS unequal angle sections. The issue is addressed herein. This paper presents an experimental investigation on both the welded and screw fastened back-to-back built-up CFS unequal angle sections under axial compression. The load-axial shortening and the load versus lateral displacement behaviour along with the deformed shapes at failure are reported. A nonlinear finite element (FE) model was then developed, which includes material non-linearity, geometric imperfections and modelling of intermediate fasteners. The FE model was validated against the experimental test results, which showed good agreement, both in terms of failure loads and deformed shapes at failure. The validated FE model was then used for the purpose of a parametric study to investigate the effect of different thicknesses, lengths and, yield stresses of steel on axial strength of back-to-back built-up CFS unequal angle sections. Five different thicknesses and seven different lengths (stub to slender columns) with two different yield stresses were investigated in the parametric study. Axial strengths obtained from the experimental tests and FE analyses were used to assess the performance of the current design guidelines as per the Direct Strength Method (DSM); obtained comparisons show that the current DSM is conservative by only 7% on average, while predicting the axial strengths of back-to-back built-up CFS unequal angle sections.

**Keywords:** axial strength; back-to-back built-up sections; buckling; cold-formed steel; finite element modelling; unequal angle sections

## 1. Introduction

The use of cold-formed steel (CFS) in construction industry has become increasingly popular over last few decades (Lian *et al.* 2017, Kyvelou *et al.* 2017, Ye *et al.* 2018a, b, Uzzaman *et al.* 2012a, b, 2017) and Lim and Nethercot (2003), and the use of back-to-back built-up CFS unequal angle sections are becoming popular as compression members. Applications of such built-up sections include struts in steel trusses and space frames, columns in portal frames and bracing members in transmission towers. In such an arrangement, welds or intermediate fasteners at discrete points along the length are used to prevent the unequal angle sections from buckling independently. The American Iron and Steel Institute (AISI) (2016) and Australian and New Zealand Standards (AS/NZS) (2018) both prescribe the modified slenderness approach to consider the spacing of fasteners in CFS built-up sections.

In the literature, no research is available on axial strength of back-to-back built-up CFS unequal angle sections under axial compression, in the arrangement shown in Fig. 1. However, research is available on back-to-back built-up CFS equal angle sections (Ananthi *et al.* 2019, Vishnuvardhan 2006). Ananthi *et al.* (2019) presented 26 experimental tests and developed a finite element (FE) model for back-to-back built-up CFS screw-fastened equal angle section columns. On the other hand, Vishnuvardhan (2006) investigated the behaviour of back-to-back built-up CFS equal angle section columns under both fixed and pinned ended boundary conditions. Other than the works reported by Ananthi *et al.* (2019) and Vishnuvardhan (2006), no work is available in the literature which investigated the axial strength of CFS built-up equal angle sections. The objective of this study was to investigate the axial strength of back-to-back screw-fastened and welded built-up CFS unequal angle section columns, which is different from the work reported by either of Ananthi *et al.* (2019) or Vishnuvardhan (2006).

In terms of CFS single angle sections under axial compression, significant research is available in the literature. Young and Chen (2008) conducted column tests on CFS non-symmetric lipped angle sections. Shi *et al.* (2011) performed experimental tests and FE analysis on the local buckling behavior of 420 MPa steel equal angle

\*Corresponding author, Ph.D. Student,  
E-mail: [kroy405@aucklanduni.ac.nz](mailto:kroy405@aucklanduni.ac.nz)

<sup>a</sup> Associate Professor, E-mail: [beulahceg@gmail.com](mailto:beulahceg@gmail.com)

<sup>b</sup> Ph.D. Student, E-mail: [bche719@aucklanduni.ac.nz](mailto:bche719@aucklanduni.ac.nz)

<sup>c</sup> Associate Professor, E-mail: [james.lim@auckland.ac.nz](mailto:james.lim@auckland.ac.nz)

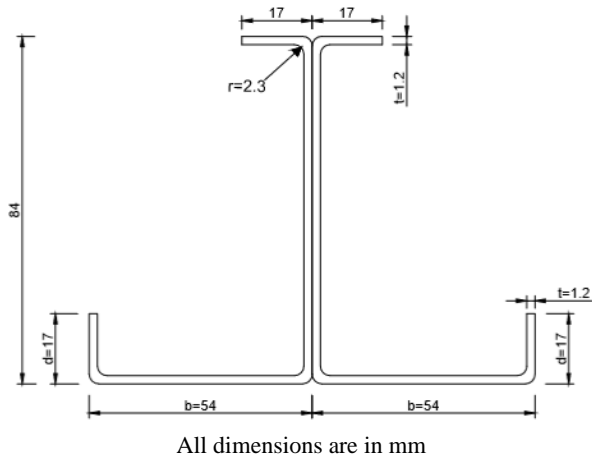


Fig. 1 Cross-sectional details of the back-to-back built-up CFS unequal angle sections investigated in this study

section columns under axial compression. Furthermore, Ellobody and Young (2007) studied the design of CFS single unequal angle sections as compression members.

For CFS built-up columns formed by connecting two back-to-back channels, extensive research has been conducted by past researchers. Dabaon *et al.* (2015) considered built-up sections, which were steel columns connecting two back-to-back channels using batten plates, it was found that both the AISI (2016) and the Eurocode (2005) were un-conservative when the steel battened columns failed through local buckling but were conservative when they failed through flexural buckling. While Stone and LaBoube (2005) investigated the axial strength of back-to-back CFS channel sections which had stiffened flanges and track sections. Whittle and Ramseyer (2009) studied the axial strength of built-up CFS channel sections, which were welded toe-to-toe. Welded channels connected back-to-back, were also investigated by Piyawat

*et al.* (2013). Zhang and Young (2012) considered back-to-back built-up CFS channel sections with edge and web stiffeners. On the other hand, Ting *et al.* (2018) investigated the effect of screw fasteners spacing on axial strength of back-to-back built-up CFS channel sections. Roy *et al.* (2018a) investigated the effect of thickness on axial strength of CFS built-up sections, by connecting two channels back-to-back, with the help of intermediate fasteners. Roy *et al.* (2018b) also investigated the axial strength of back-to-back gapped built-up CFS channel sections and proposed design recommendations for such gapped built-up columns. The gap was formed between the two back-to-back channels with the help of link-channels (Roy *et al.* 2018b. More recently, Roy *et al.* (2019a) studied the axial strength of face-to-face built-up CFS channel sections and showed that AISI (2016) and AS/NZS (2018) is generally conservative for built-up columns failed through global buckling; however, the AISI (2016) and AS/NZS (2018) can be un-conservative for columns that failed by local buckling.

Other works include that of Fratamico *et al.* (2016) and Anbarasu *et al.* (2015) who investigated the axial strength of sheathed and bare built-up CFS columns and CFS web stiffened built-up batten columns, respectively. Lu *et al.* (2017) conducted experimental tests and developed a novel direct strength method for the design of CFS built-up I section columns. On the other hand, Reyes and Guzmanc (2011) investigated the axial strength of CFS built-up welded box sections. Recently, Roy *et al.* (2018c), studied the axial strength of back-to-back built-up CFS un-lipped channels under axial compression and reported that AISI (2016) and AS/NZS (2018) can be un-conservative by around 8% for columns which failed through local buckling. In case of the CFS built-up columns composed of zed-sections, Georgieva *et al.* (2012) considered such built-up columns which were connected toe-to-toe. A new approach for the design of double-zed CFS members based on the direct strength method was proposed by Georgieva *et al.* (2012).

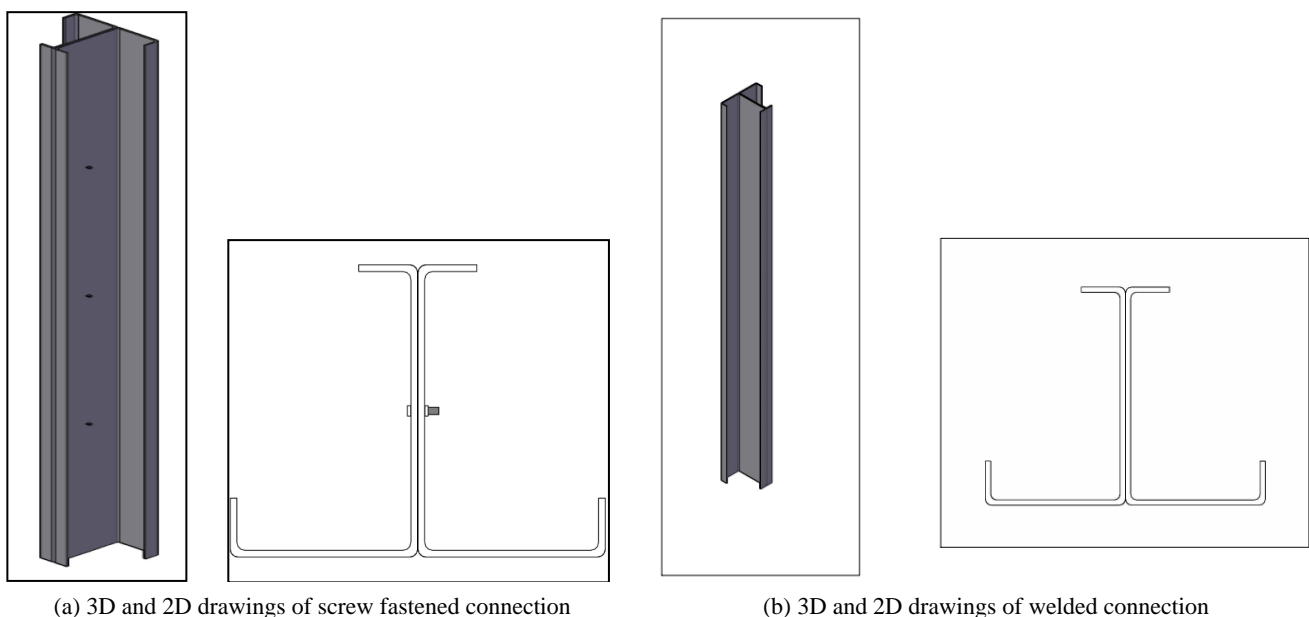


Fig. 2 General arrangements of the back-to-back built-up CFS unequal angle sections investigated in this study

From the literature review, it appears that not even a single research is available on axial strength of back-to-back built-up CFS unequal angle section columns with different screw fastener spacing. The issue is addressed experimentally and numerically herein.

This paper presents an experimental investigation on axial strength of back-to-back built-up CFS unequal angle sections (Fig. 2). Both the screw fastened and welded built-up sections were tested. The cross-section of the single unequal angles studied by Ellobody and Young (2007) under compression, are chosen for this study to connect the unequal angles back-to-back and to form the built-up columns. The material properties of the test specimens were determined by tensile coupon tests. The effect of length, load-axial shortening, and failure modes of the back-to-back built-up CFS unequal angle section columns were investigated.

A non-linear FE model was also developed, which includes material non-linearity, geometric imperfections and modelling of intermediate fasteners. The FE model was validated against the experimental test results of back-to-back built-up CFS unequal angle section columns. Additionally, another FE model was developed for back-to-back built-up CFS equal angle section columns and validated against the test results of back-to-back built-up CFS equal angle section columns, reported by Vishnuvardhan (2006). The purpose of developing the FE model for built-up equal angle section columns was to confirm the reliability of the modelling technique applied in this study. This is to be mentioned that the modelling technique adopted for both the back-to-back built-up CFS equal and unequal angle section columns were exactly the same and the further validation of the FE model for equal angle sections against the test results of Vishnuvardhan (2006), indicated that the FE model can predict the failure behavior of both the equal and unequal angle built-up columns.

Using the validated FE model, a parametric study was conducted for back-to-back built-up CFS unequal angle sections, comprising 70 models, varying the length of the built-up columns from 250 mm to 3000 mm (stub to slender

columns), thicknesses from 0.55 mm to 5 mm with two different yield stresses of steel (250 MPa and 550 Mpa). The axial strengths obtained from the experimental tests and parametric analysis were used to assess the performance of the current design guidelines as per the Direct Strength Method (DSM), while predicting the axial strength of back-to-back built-up CFS unequal angle section columns.

This paper has therefore presented the details of the experimental and FE investigations and their results are reported along with the comparison of axial strengths obtained from the experiments, FEA and the current design guidelines for back-to-back built-up CFS unequal angle section columns.

## 2. Experimental investigation

### 2.1 Experimental tests on back-to-back built-up CFS unequal angle section columns

#### 2.1.1 Test specimens

Fig. 1 shows the cross-sectional details of the built-up section (BA84) considered in the experimental investigation, where two unequal angle sections were connected back-to-back. Two types of connections were used to connect the back-to-back unequal angle sections: screw fasteners and stich welding. For screw fasteners, a spacing of 200 mm was used to connect the unequal angle sections. On the other hand, for built-up sections connected by stich welding, 50 mm weld spacing was used to connect the angle sections back-to-back (Fig. 2). All the columns had lengths of 500 mm. The dimensions of the test specimens along with the type of connections (screw fastened or welded) are given in Table 1. The spacing of the screw fasteners was designed to cover the spacing requirements of CFS built-up columns as per the AISI (2016) standard.

#### 2.1.2 Section labels

The built-up sections were labelled in such a way that the type of section, cross-sectional dimensions of the

Table 1 Axial strength of the back-to-back built-up CFS unequal angle section columns from experiments, FEA and the current design standards (DSM)

Specimen	First leg width	Second leg width	Lip depth	Thickness	Length	Spacing	Test results	FEA results		Current DSM design strengths	
	d <sub>1</sub>	d <sub>2</sub>	d <sub>3</sub>	t	L	S	P <sub>EXP</sub>	P <sub>FEA</sub>	P <sub>EXP</sub> /P <sub>FEA</sub>	P <sub>DSM</sub>	P <sub>EXP</sub> /P <sub>DSM</sub>
	(mm)	(mm)	(mm)	(mm)	(mm)	(mm)	(kN)	(kN)	-	(kN)	-
<b>Screw fastened</b>											
BA84-d17-t1.2-S200-1	83.6	53.5	17.0	1.21	500	200.0	69.9	71.5	0.96	69.2	0.98
BA84-d17-t1.2-S200-2	82.7	54.0	16.7	1.19	500	200.0	67.0	69.8	0.94	68.4	0.96
<b>Welded</b>											
BA84-d17-t1.2-WS50-1	83.6	54.0	16.8	1.18	500	50.0	74.2	79.6	0.98	68.3	1.04
BA84-d17-t1.2-WS50-2	82.5	53.5	16.9	1.17	500	50.0	72.4	77.4	1.03	69.5	1.06
Mean	-	-	-	-	-	-	-	-	0.95	-	1.03
COV	-	-	-	-	-	-	-	-	0.02	-	0.04

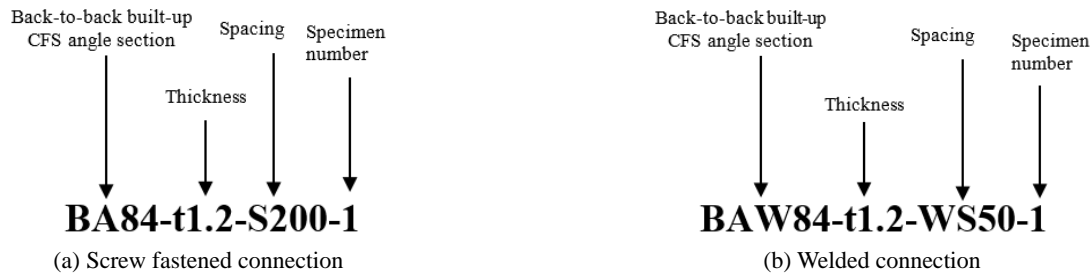


Fig. 3 Specimen labelling for back-to-back built-up CFS unequal angle section columnst

angle sections, thickness of steel, length of the columns and type of connections (screw fastened or welded) were expressed by the label. Fig. 3 shows the examples of the labelling used in the experimental program for both screw-fastened and welded back-to-back built-up CFS unequal angle section columns. As shown in Fig. 3(a), the label BA84-t1.2-S200-1 can be explained as follows:

- “BA84” indicates the back-to-back built-up CFS unequal angle sections with 84 mm vertical leg width, 54 mm horizontal leg width and 17 mm lip depth.
- “t1.2” indicates the thickness of steel used as 1.2 mm.
- “S200” indicates the nominal screw fastener spacing of 200 mm.
- “1” indicates the specimen number as 1.

On the other hand, for welded back-to-back built-up CFS angle section columns, the label, BAW84-t1.2-WS50-1 is shown in Fig. 3(b) and can be explained as follows:

- “BAW84” indicates back-to-back built-up CFS

unequal angle section columns connected by stich welding with 84 mm vertical leg width, 54 mm horizontal leg width and 17 mm lip depth.

- “t1.2” indicates the thickness of steel used as 1.2 mm.
- “WS50” indicates the stich welding spacing of 50 mm.
- “1” indicates the specimen number as 1.

### 2.1.3 Material testing

Tensile coupon tests were conducted to determine the material properties of the test specimens. The tensile coupons were cut from the center of the back-to-back built-up unequal angle sections tested herein, in accordance with the ASTM A 370–92 (1996). Each of three coupons were cut from the longitudinal directions of the vertical and horizontal legs of 1.2 mm thick unequal angle sections. The coupons were tested in an UTM (Universal Testing Machine) which has a capacity of 500 kN. From the results of the tensile coupon tests, the average values of the Young’s modulus and yield strength were 205 GPa and 231.42 MPa, respectively (Table 2) for 1.2 mm thick unequal angle sections (Fig. 4).

Table 2 Material properties obtained from the tensile coupon tests

Section	Nominal thickness	Base metal thickness	Gauge length	Yield stress	Gauge width	Ultimate stress	Percentage elongation	Young’s Modulus
	t	T	L <sub>o</sub>	$\sigma_{0.2}$	b	F <sub>u</sub>	-	E
	(mm)	(mm)	(mm)	(Mpa)	-	(Mpa)	-	(Gpa)
Longitudinal	1.2	1.2	50	231.42	12.49	308.89	34.60	205

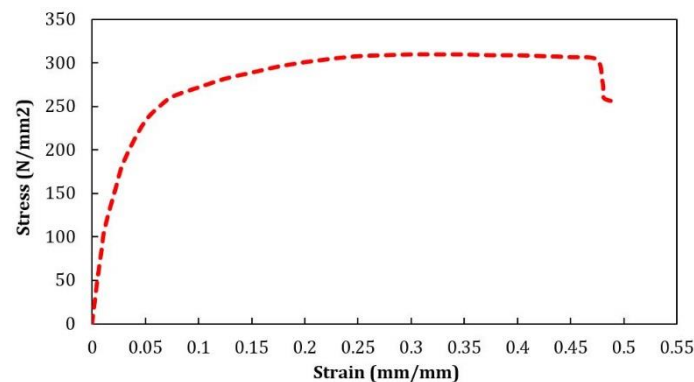


Fig. 4 Full stress-strain curve of the CFS used in this research

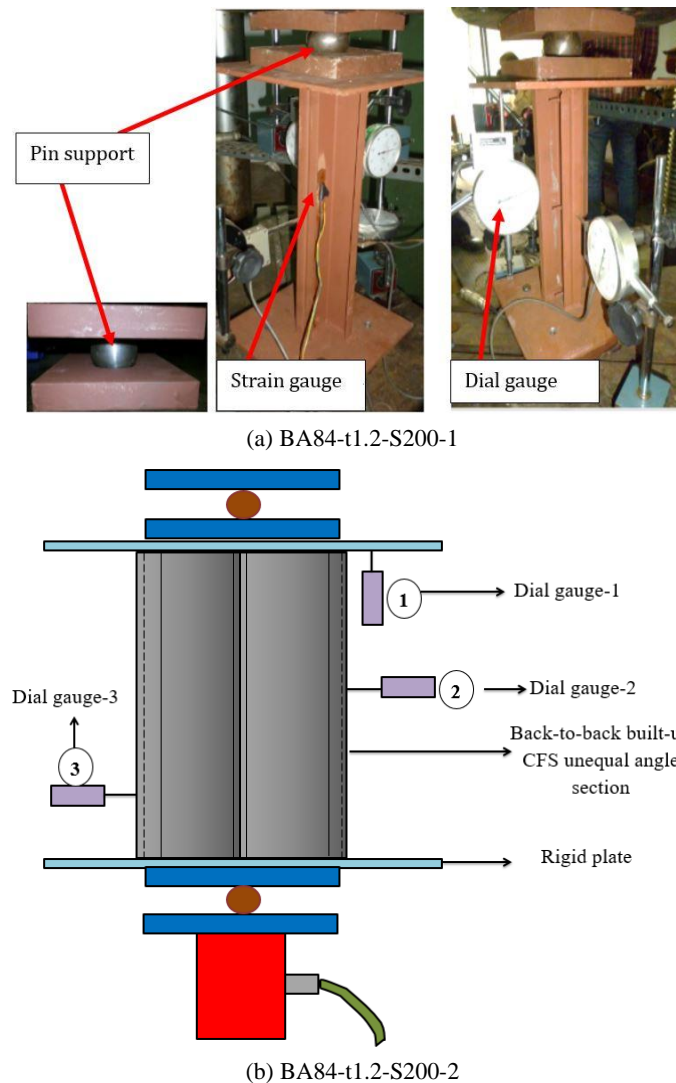


Fig. 5 Photograph of experimental test set-up

#### 2.1.4 Testing-rig and loading procedure

A Compression Testing Machine (CTM), which has a capacity of 500 kN, was used to apply the axial load on back-to-back built-up CFS unequal angle sections. The specimens were first placed on top of the base plates, and the verticality of the specimens was roughly checked using a spirit level along the legs of the angle sections. Back-to-back built-up CFS unequal angle sections were tested under pinned ended boundary conditions. To simulate the pin ended boundaries, two base plates (120 mm × 120 mm) of 12 mm thickness were used (Fig. 5). The top base plate, through which the load was transferred to the specimen was machined for even surface and was welded in such a way that the centre of gravity of the top base plate coincides with the point of loading of the specimen. The specimen was brought to the negligible torsional imperfection and minimum possible lateral deflection by twisting and pulling the specimen without making any permanent deformation. The jack was lowered to clamp the specimen and once again the imperfections were measured using a spirit level. The external load cell was placed at the bottom of the built-up column. Three dial gauges were used for each test. Dial

gauge positions are numbered as 1, 2 and 3, as shown in Fig. 5. Dial gauge-1 was used to determine the axial shortening and dial gauge-2 and 3 were used to determine the lateral displacements at the mid-height and one third height of the columns from the bottom base plate, respectively. The displacement control method was used to apply the axial load to the columns. The benefit of using the displacement control is that, it can predict the post-buckling behaviour of the built-up columns. The loading rate of 0.35 mm/min at an increment of 1/10 of the ultimate load. The dial gauges and load cell readings were recorded after each increment of loading. The specimens were loaded to the maximum limit beyond which there was a rapid increase in strain gauge and dial gauge readings with no increase in the axial load.

#### 2.1.5 Experimental results

The axial strengths determined from the experiments ( $P_{EXP}$ ) are shown in Table 1 for both the screw fastened and welded back-to-back built-up CFS unequal angle section columns. As can be seen from Table 1, the axial strength of welded back-to-back built-up CFS unequal angle sections is

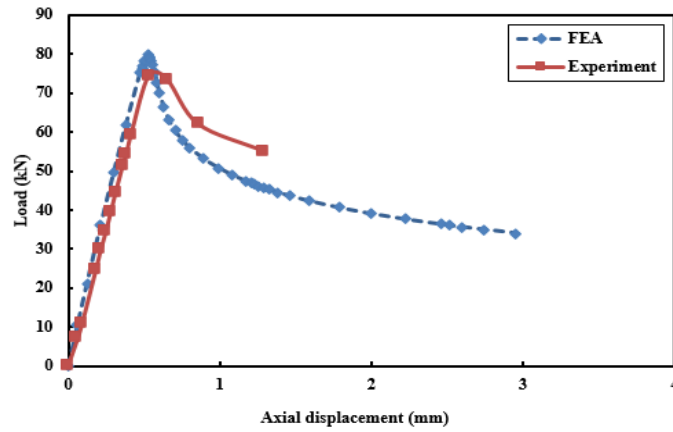


Fig. 6 Load versus axial displacement curves for BAW84-t1.2-WS50-1

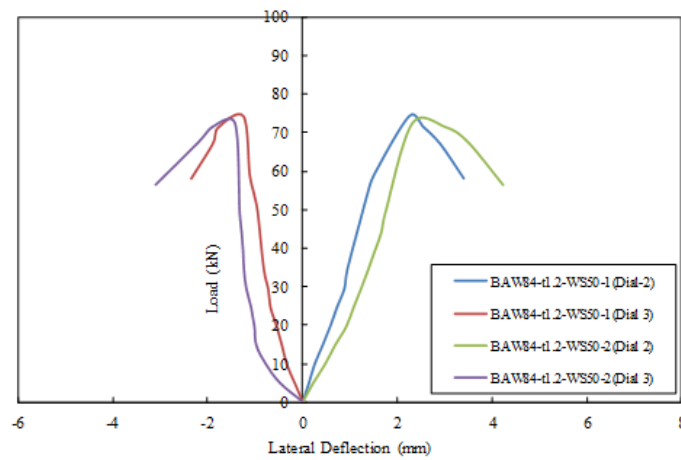


Fig. 7 Load versus lateral displacement curves from the tests



(a) BA84-t1.2-S200-1



(b) BA84-t1.2-S200-2



(c) BAW84-t1.2-WS50-1



(d) BAW84-t1.2-WS50-2

Fig. 8 Photograph of the back-to-back built-up CFS unequal angle section columns at failure from experiments

higher (around 7%) than the screw fastened built-up CFS unequal angle section columns, for the same cross-sectional dimensions and thicknesses of the built-up columns.

The load-axial shortening relationship for BAW84-t1.2-WS50-1 is plotted in Fig. 6. It is shown that the relationship is almost linear up to a load of 68 kN, which is 92% of the ultimate failure load for BAW84-t1.2-WS50-1. After that,

the non-linear behavior is continued until the failure load is reached, which is 74.20 kN.

Fig. 7 shows the load versus lateral displacement behaviour for BAW84-t1.2-WS50-1 at mid-height and at one third height from the bottom base plate. As can be seen from Fig. 7, the rate of increase of mid-height lateral displacements was higher at initial stage of loading, when compared to the lateral displacements at one-third height of

the column. In the experimental tests, all columns including screw fastened and welded built-up CFS unequal angle sections, failed through local buckling except for BA84-t1.2-S200-2 which showed a combination of local and flexural buckling. Fig. 8 shows the failure modes observed during experimental tests for both the screw fastened and welded back-to-back built-up CFS unequal angle section columns.

Table 3 Comparison of axial strength from FEA, experimental results (Vishnuvardhan (2006)) and the current DSM for back-to-back built-up CFS equal angle section columns

Specimen	Leg width	Lip depth	Thickness	Length	Tests results P <sub>EXP</sub> (kN)	FEA results		Current DSM design strengths		Failure modes
	d <sub>1</sub> / d <sub>2</sub> mm	d <sub>3</sub> (mm)	t (mm)	L (mm)		P <sub>FEA</sub> (kN)	P <sub>EXP</sub> / P <sub>FEA</sub> -	P <sub>DSM</sub> (kN)	P <sub>EXP</sub> /P <sub>DSM</sub> -	
<b>Pin-pin end conditions</b>	-	-	-	-	-	-	-	-	-	-
BA30-d20-t2-λ15	30	20	2.00	164	89.7	86.9	1.03	73.1	1.23	L+FT
BA30-d20-t2-λ20	30	20	2.00	219	84.3	79.9	1.06	72.6	1.16	L+ FT
BA30-d20-t2-λ25	30	20	2.00	274	80.8	78.5	1.03	71.7	1.13	L+F
BA30-d20-t2-λ30	30	20	2.00	329	66.8	71.3	0.94	70.8	0.95	L+F
BA35-d15-t2-λ15	35	15	2.00	189	85.3	80.2	1.06	72.5	1.18	L+ FT
BA35-d15-t2-λ20	35	15	2.00	252	82.1	80.1	1.03	71.5	1.15	L+ FT
BA35-d15-t2-λ25	35	15	2.00	315	81.1	79.5	1.02	70.4	1.15	L+F
BA35-d15-t2-λ30	35	15	2.00	378	74.6	78.6	0.95	68.9	1.08	L+F
BA40-d15-t2-λ15	40	15	2.00	215	121.9	128.6	0.95	158.8	0.77	L+ FT
BA40-d15-t2-λ30	40	15	2.00	429	110.3	114.5	0.96	141.4	0.78	L+ FT
BA40-d15-t3.15-λ15	40	15	3.15	207	189.2	188.5	1.00	144.7	1.30	L+F
BA40-d15-t3.15-λ30	40	15	3.15	276	168.7	169.8	0.99	142.1	1.24	L+F
BA60-d15-t2-λ20	60	15	2.00	426	136.6	142.9	0.96	150.5	0.91	L
BA60-d15-t2-λ30	60	15	2.00	638	127.1	137.2	0.93	130.7	0.97	L+ FT
BA60-d15-t3.15-λ20	60	15	3.15	414	216.3	217.2	1.00	190.5	1.14	L
BA60-d15-t3.15-λ30	60	15	3.15	621	138.9	145.1	0.96	172.8	0.80	L+ FT
BA60-d25-t2-λ20	60	25	2.00	443	140.7	148.4	0.95	190.2	0.74	L
BA60-d25-t2-λ30	60	25	2.00	665	131.7	137.8	0.96	179.0	0.74	L+ FT
BA60-d25-t3.15-λ20	60	25	3.15	432	254.1	259.6	0.98	234.2	1.09	L
BA60-d25-t3.15-λ30	60	25	3.15	648	235.4	238.9	0.99	224.4	1.04	L+ FT
BA70-d15-t3.15-λ20	70	15	2.00	482	220.7	224.7	0.98	210.0	1.05	L
BA70-d15-t3.15-λ30	70	15	2.00	722	147.4	152.1	0.97	185.5	0.79	L+ FT
BA70-d25-t3.15 λ20	70	25	2.00	503	295.8	290.2	1.02	261.4	1.13	L
BA70-d25-t3.15-λ30	70	25	2.00	755	286.3	280.6	1.02	246.2	1.16	L+ FT
<b>Fix-fix end conditions</b>	-	-	-	-	-	-	-	-	-	-
BA40-d10-t2-λ10	40	10	2.00	180	77.5	80.1	0.97	70.5	1.08	L+ FT
BA40-d10-t2-λ15	40	10	2.00	270	70.0	73.3	0.96	66.9	1.00	L+ FT
BA40-d10-t2-λ20	40	10	2.00	360	62.5	66.3	0.94	63.1	0.93	L
Mean	-	-	-	-	-	-	0.98	-	1.03	-
COV	-	-	-	-	-	-	0.04	-	0.16	-

\*L- Local buckling; FT- Flexural-torsional buckling; F-Flexural buckling

## 2.2 Summary of experimental tests on axial strength of back-to-back built-up CFS equal angle section columns from Vishnuvardhan (2006)

In order to compare the axial strengths of back-to-back built-up CFS equal and unequal angle sections, the test results of Vishnuvardhan (2006) for back-to-back built-up CFS equal angle sections were used in this paper. In total, 27 tests were reported by Vishnuvardhan (2006) for axial strengths of back-to-back built-up CFS equal angles. The test specimens were labelled in such a way that the cross-sectional dimensions, thickness of the angle sections and slenderness of the built-up sections were defined by the label. A typical specimen label, BA70-d25-t3.15-λ30 can be explained as follows:

- “BA70” indicates the back-to-back built-up CFS equal angle sections with 70 mm vertical leg width, 70 mm horizontal leg width and 25 mm lip depth.
- “t3.15” indicates the thickness of steel as 1.2 mm.
- “λ30” indicates the slenderness ratio as 30.

For the compression testing, the load was applied axially to the specimens via a Column Testing Machine (CTM), which had a capacity of 2000 kN. The axial strengths of the built-up equal angle section columns from Vishnuvardhan (2006) are shown in Table 3. These test results were used for validating the FE model described in section 3 for back-to-back built-up CFS equal angle section columns. Further details of the experimental tests on back-to-back built-up CFS equal angle section columns can be found in Vishnuvardhan (2006).

## 3. Finite element investigation

### 3.1 General

ABAQUS (2018) was used to develop a non-linear elasto-plastic FE models for both the back-to-back built-up CFS equal and unequal angle sections under axial compression. The FE models were based on the centerline dimensions of the cross-section of built-up angle sections. Two types of FE analysis were performed. The buckling modes of the built-up columns were determined, first, through the eigenvalue analysis, which is a linear elastic analysis performed using the (\*BUCKLE) procedure available in the ABAQUS library. A load-displacement nonlinear analysis was then carried out using RIKS algorithm available in the ABAQUS library. The geometric imperfections and material nonlinearities were included in the FE model. Specific modeling issues are described in the following sections.

### 3.2 Geometry and material properties

The full geometry of both the back-to-back built-up CFS equal and unequal angle sections was modelled. True values of stresses and strains were specified in the FE model to incorporate the material non-linearities. The ABAQUS

classical metal plasticity model was used for the analysis and validation purposes. Isotropic yielding, associated plastic flow theory, and isotropic hardening behavior was considered in the FE models. For the parametric study (described in section 5 of this paper), a simplified elastic perfectly plastic stress-strain curve obeying Von Mises yield criterion was used. The yield stress, ultimate stress, along with Young’s modulus values were considered from the results of the coupon tests described in the experimental section of this paper (section 2.1.3) for back-to-back built-up unequal angle sections. Whereas the material properties of the back-to-back built-up CFS equal angle sections were taken from Vishnuvardhan (2006). Following the recommendation given in the ABAQUS manual, the engineering material curves were converted into the true material curves in the FE analysis by using the following equations

$$\sigma_{true} = \sigma(1 + \varepsilon) \quad (1)$$

$$\varepsilon_{true(pl)} = \ln(1 + \varepsilon) - \frac{\sigma_{true}}{E} \quad (2)$$

Where  $E$  is the Young’s Modulus,  $\sigma$  and  $\varepsilon$  are the engineering stress and strain, respectively.

### 3.3 Element type and finite element mesh

A linear 4-noded quadrilateral thin shell element (S4R5), available in ABAQUS element library, was used to model both the equal and unequal angle sections, connected back-to-back. A mesh size of 5 mm × 5 mm (length×width) was used for the convergence of the FE models. Along the length of the sections, the number of elements was chosen so that the aspect ratio of the elements was close to one. A mesh sensitivity analysis was performed to verify the

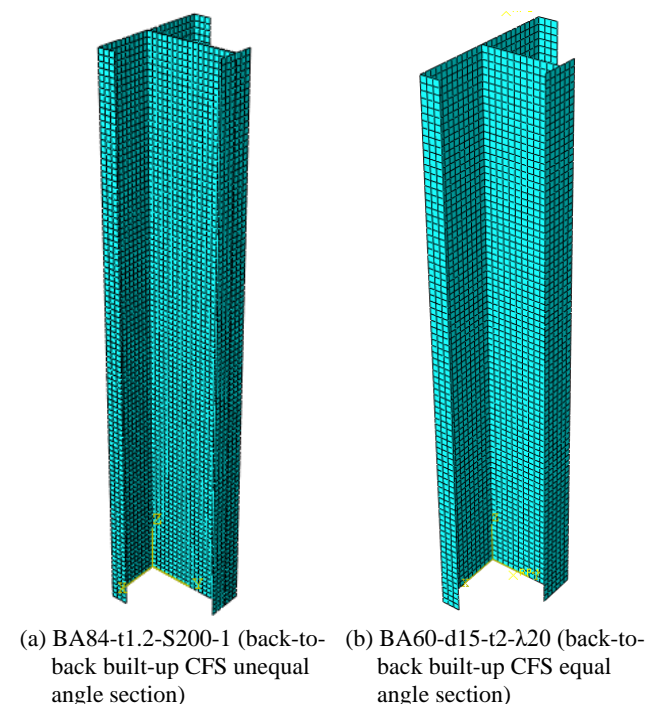


Fig. 9 FE meshing

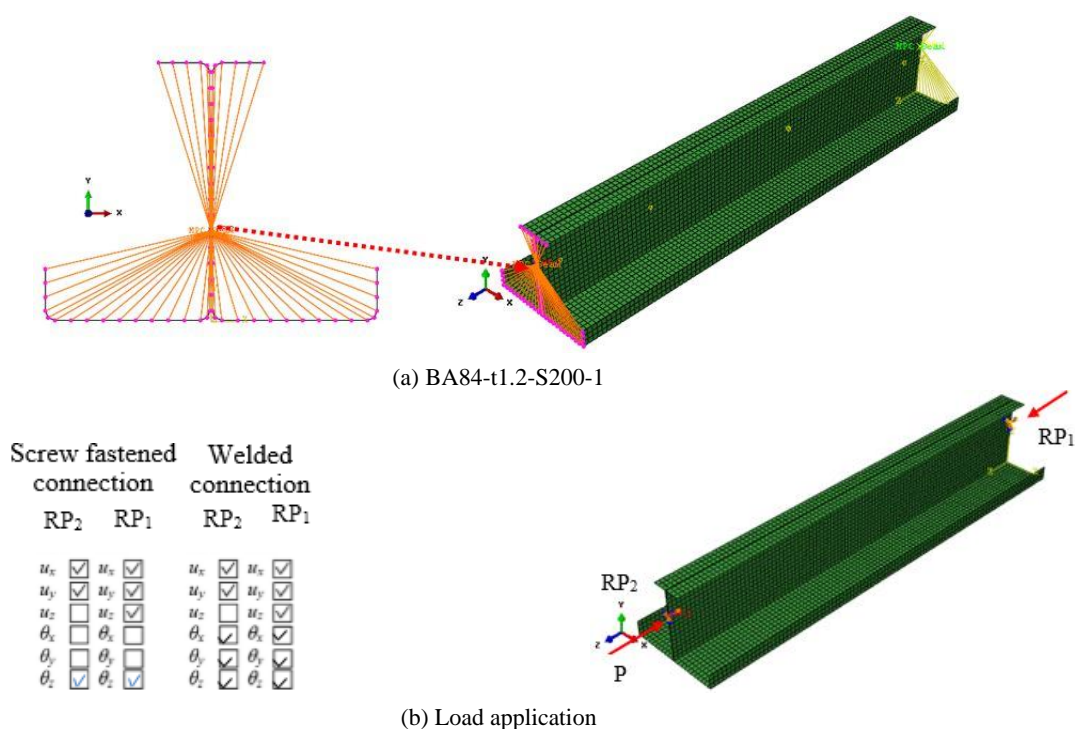


Fig. 10 Details of the FE model for BA84-t1.2-S200-1

number of elements for both the FE models of CFS built-up equal and unequal angle sections. The typical FE meshes of back-to-back built-up CFS unequal and equal angle sections are shown in Figs. 9(a) and (b), respectively.

### 3.4 Boundary conditions and load application

Pin-ended boundary conditions were applied for all built-up equal and unequal angle section columns. In order to simulate pin-ended boundary conditions, displacements and rotations were applied to the upper and lower ends of the back-to-back built-up CFS angle sections through the reference points. The reference point was considered as the center of gravity (CG) of the cross-section of the back-to-back built-up CFS angle sections. The screw fasteners between the back-to-back built-up CFS equal and unequal angle sections were modelled using the MPC beam connector elements available in the ABAQUS library (Fig. 10(a)). The load was applied to the reference points of both the built-up equal and unequal angle sections as shown in Fig. 10(b). The RIKS algorithm, available in the ABAQUS library, was used to apply the load in increments. By using the RIKS method, post buckling behaviour of the back-to-back built-up columns can be captured (Roy *et al.* 2018d).

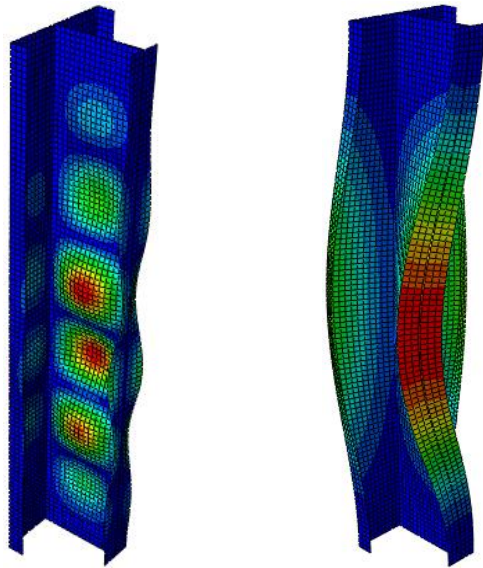
### 3.5 Contact modelling

“Surface to surface” contact was used for modeling the interaction between the legs of the back-to-back built-up CFS unequal angle sections. The leg of one angle section was modeled as slave surface, while the leg of another angle section was considered as master surface. There was no penetration between the two contact surfaces. Similar

modelling technique was used to model the contact surface between the legs of back-to-back built-up CFS equal angle sections.

### 3.6 Modelling of initial imperfections

Local, distortional and flexural buckling behavior of the back-to-back built-up CFS equal and unequal angle sections depends on many factors such as: Depth of angle-thickness ratio ( $D/t$ ), width of angle-thickness ratio ( $b/t$ ), slenderness around  $x$  and  $y$  axis and spacing of intermediate fasteners. The initial imperfections are caused in compression members as a result of the fabrication process. Distortional buckling is one of the important modes of buckling for CFS members and can be critical failure modes for angle sections. Therefore, along with local and overall imperfections, distortional imperfections were also considered in the FE models of back-to-back built-up CFS equal and unequal angle section columns. The local, distortional and overall buckling modes were superimposed for accurate FE analysis. Eigenvalue analyses of the built-up columns were performed with very small to large angle thickness to determine the contours for the local, distortional and overall imperfections. The lowest buckling mode (Eigen mode 1) in ABAQUS (2018), was used as the shape of local and overall buckling modes. The magnitudes of the local, distortional and global imperfections were considered as  $0.006 * w * t$ ,  $1.0 * t$  and  $1/1000$  of the full length of the column, respectively, following the recommendations of Schafer and Pekoz (1998). The contours of the local and flexural buckling modes obtained from the eigen value analyses are shown in Figs. 11(a) and (b), for BA84-t1.2-S200-1.



(a) Local buckling for BA84-t1.2-S200-1 (b) Flexural buckling for BA84-t1.2-S200-1

Fig. 11 Initial imperfection contours from the FEA

### 3.7 Modelling of residual stresses

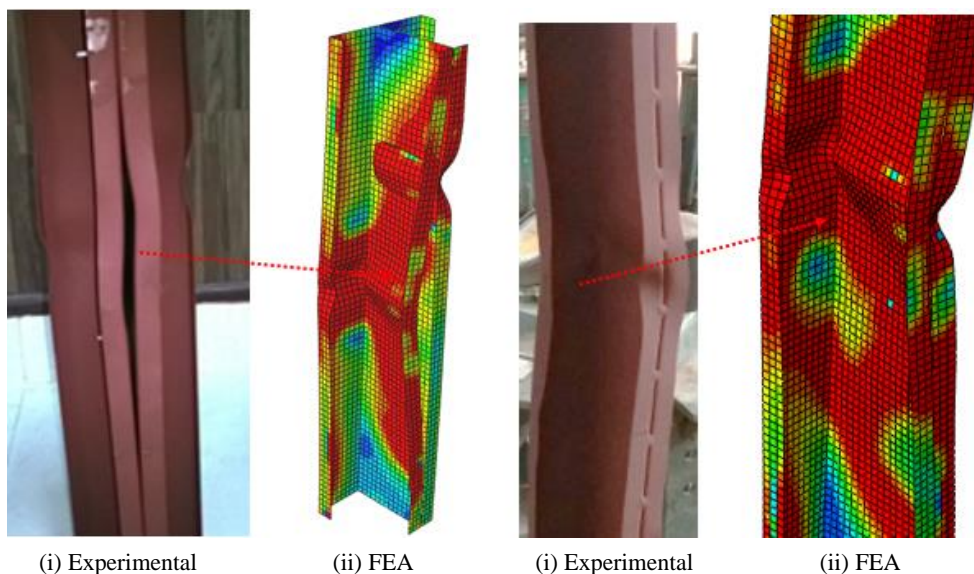
Residual stresses can be incorporated into the FE models of built-up equal and unequal angle section columns, as initial state using the ABAQUS (\*INITIAL CONDITIONS, TYPE = STRESS) option. However, previous studies detailed in Roy *et al.* (2018d), Schafer and Pekoz (1998) showed that it has a negligible effect on the column strength, stiffness of the built-up column, load-axial shortening behaviour and failure modes. Therefore, residual stresses were not included in any of the FE models for back-to-back built-up CFS equal and unequal angle section columns, to avoid the complexity of the analysis.

### 3.8 Validation of the finite element models

In order to validate the FE models, the test results presented in section 2 were compared against the results of FEA as shown in Tables 1 and 3 for built-up unequal and equal angles, respectively. As can be seen from Table 1, the mean value of the ratios of  $P_{EXP}/P_{FEA}$  for back-to-back built-up CFS unequal angle sections (both screw-fastened and welded) is 0.95; with a co-efficient of variation (COV) of 0.02. Besides, the load-axial shortening behavior of the BAW84-t1.2-WS50-1 is plotted in Fig. 6 from both the experiments and FEA. It is shown that the relationship was almost linear up to the ultimate load of 79.66 kN, for welded connection of BAW84-t1.2-WS50-1 after which the non-linear behavior was observed, from the FEA. Similar behavior was observed for other back-to-back built-up CFS unequal angle section columns. As can be seen from Fig. 6, close agreement is achieved between the experiments and FE results, both in terms of ultimate load and initial stiffness. Also, the experimental buckling modes are similar to the buckling modes obtained from the FEA for both the screw-fastened and welded back-to-back built-up CFS unequal angle section columns (Fig. 12).

The axial strengths obtained from the experimental tests reported by Vishnuvardhan (2006) and the FEA described in this study are compared in Table 3 for back-to-back built-up CFS equal angle section columns. As shown in Table 3, the mean value of the ratios of  $P_{EXP}/P_{FEA}$  is 0.98, with a COV of 0.04 for axial strengths of back-to-back built-up CFS equal angle section columns. Besides, the failure modes obtained from the experiments (Vishnuvardhan 2006) and the FEA reported herein, are compared in Fig. 13 for BA70-d25-t3.15-λ30.

As shown in Tables 1 and 3, the experimental and FEA results show good agreement for both the ultimate strength and the failure modes for back-to-back built-up CFS unequal and equal angle section columns, respectively. The validated FE model for back-to-back built-up CFS unequal



(i) Experimental (ii) FEA (a) Self drilling screw fastened column (BA84-t1.2-S200-1) (b) Stich welded column (BAW84-t1.2-WS50-2)

Fig. 12 Failure modes of back-to-back built-up unequal angle sections

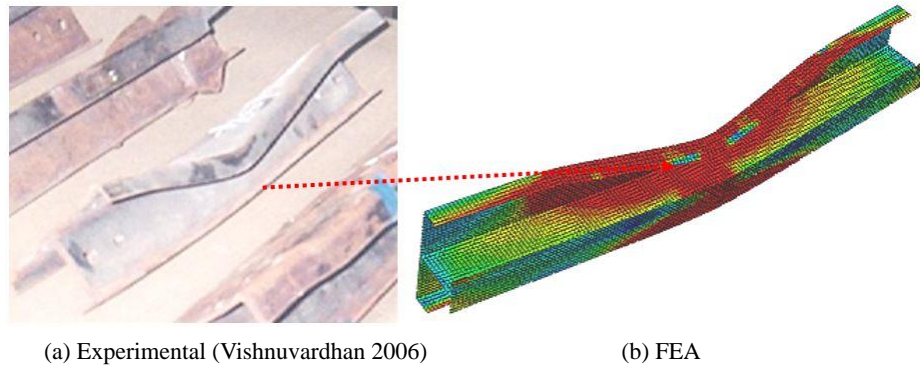


Fig. 13 Failure modes of back-to-back built-up equal angle section for BA70-d25-t3.15-λ30

angle section column was further used for the purpose of an extensive parametric study as described in section 5 of this paper.

#### 4. Design guidelines in accordance with the AISI and AS/NZ standards

The un-factored design strengths of back-to-back built-up CFS angle sections can be calculated in accordance with the American Iron and Steel Institute's specification (AISI 2016) and the Australia/New Zealand standards (AS/NZS 2018). The AISI (2016) and AS/NZS (2018) recommend the use of both the Effective Width Method (EWM) and the Direct Strength Method (DSM) to calculate the buckling strength and the design strength of CFS columns. The DSM was used in this study to calculate the design strengths of back-to-back built-up CFS unequal and equal angle section columns. For both the back to-back built-up CFS equal and unequal angle sections, the un-factored design strength of axially loaded compression members can be calculated in accordance with the AISI (2016) & AS/NZS (2018), following the design equations given below

$$P_{\text{AISI\&AS/NZS}} = A_e F_n \quad (3)$$

The critical buckling stress ( $F_n$ ) can be calculated using the Eqs. (4) and (5) as follows

$$\text{For } \lambda_c \leq 1.5, F_n = (0.658\lambda_c^2) F_y \quad (4)$$

$$\text{For } \lambda_c > 1.5, F_n = \left(\frac{0.877}{\lambda_c^2}\right) F_y \quad (5)$$

The non-dimensional critical slenderness ( $\lambda_c$ ) can be calculated as using Eq. (6) as given below

$$\lambda_c = \sqrt{\frac{F_y}{F_e}} \quad (6)$$

According to the AISI (2016) and AS/NZS (2018), the modified slenderness ratio can be calculated as per the Eq. (7)

$$\left(\frac{KL}{r}\right)_m = \sqrt{\left(\frac{KL}{r}\right)_o^2 + \left(\frac{S}{r_i}\right)^2} \quad (7)$$

When,  $\left(\frac{S}{r_i}\right) \leq 0.5 \left(\frac{KL}{r}\right)_o$

- $\left(\frac{KL}{r}\right)_o$  - Overall slenderness ratio of the built-up section
- S - Spacing between the intermediate fasteners
- $r_i$  - Minimum radius of gyration of a single angle section.
- K - Effective length factor
- L - Unbraced member length

The nominal axial strength or un-factored design strength ( $P_{\text{DSM}}$ ) is the minimum of the nominal axial strengths for flexural buckling ( $P_{ne}$ ), local buckling ( $P_{nl}$ ), and distortional buckling ( $P_{nd}$ ), as shown in Eq. (8).

$$P_{\text{DSM}} = \min(P_{ne}, P_{nl}, P_{nd}) \quad (8)$$

The nominal axial strength ( $P_{ne}$ ) for flexural buckling can be calculated using Eq. (9).

$$P_{ne} = \begin{cases} (0.658\lambda_c^2) P_y & \text{for } \lambda_c \leq 1.5 \\ \left(\frac{0.877}{\lambda_c^2}\right) P_y & \text{for } \lambda_c > 1.5 \end{cases} \quad (9)$$

Where,  $\lambda_c = \sqrt{P_y/P_{cre}}$  and  $P_y = Af_y$

$P_y$  is the squash load;

A is the gross cross-sectional area;

$f_y$  is the yield stress, which is the static 0.2% proof stress ( $\sigma_{0.2}$ );

$P_{cre}$  is the critical elastic column buckling load in flexural buckling in this study.

The nominal axial strength for local buckling ( $P_{nl}$ ) can be calculated by using Eq. (10).

$$P_{nl} = \begin{cases} P_{ne} & \text{for } \lambda_1 \leq 0.776 \\ \left[1 - 0.15 \left(\frac{P_{cri}}{P_{ne}}\right)^{0.4}\right] \left(\frac{P_{cri}}{P_{ne}}\right)^{0.4} P_{ne} & \text{for } \lambda_1 > 0.776 \end{cases} \quad (10)$$

Where  $\lambda_1 = \sqrt{P_{ne}/P_{cri}}$  and,  $P_{cri} = Af_{oi}$ .

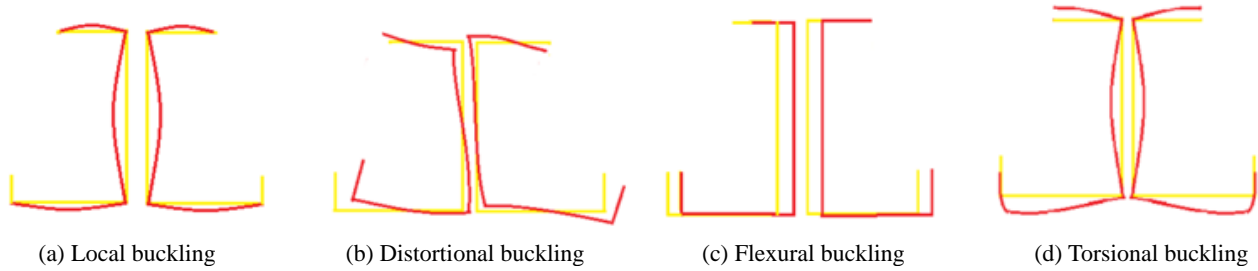


Fig. 14 Various buckling patterns of back-to-back built-up CFS unequal angle sections (CUFSM 2018)

Table 4 Comparison of axial strengths from FEA and the current DSM for back-to-back built-up CFS unequal angle section columns

Specimen	First leg width	Second leg width	Lip depth	$F_y$	Thickness	Length	Screw spacing	FEA Results	Current DSM design strengths	Comparison	Failure modes
	$d_1$	$d_2$	$d_3$	-	$t$	$L$	-	$P_{FEA}$	$P_{DSM}$	$P_{FEA}/P_{DSM}$	-
	(mm)	(mm)	(mm)	MPa	(mm)	(mm)	(mm)	(kN)	(kN)	-	-
<b>BA-t0.55</b>											
BA84-t0.55-S75	84	54	17	250	0.55	250	75	18.3	15.4	1.19	L
BA84-t0.55-S75	84	54	17	550	0.55	250	75	27.0	22.3	1.21	L+F
BA84-t0.55-S175	84	54	17	250	0.55	625	175	17.0	14.3	1.19	L
BA84-t0.55-S175	84	54	17	550	0.55	625	175	26.1	21.9	1.20	L+FT
BA84-t0.55-S225	84	54	17	250	0.55	1000	225	16.3	14.2	1.15	L+FT
BA84-t0.55-S225	84	54	17	550	0.55	1000	225	19.3	17.6	1.10	L+FT
BA84-t0.55-S350	84	54	17	250	0.55	1500	350	12.1	10.3	1.17	L+FT
BA84-t0.55-S350	84	54	17	550	0.55	1500	350	13.1	11.3	1.15	L+FT
BA84-t0.55-S475	84	54	17	250	0.55	2000	475	8.2	7.3	1.12	L+FT
BA84-t0.55-S475	84	54	17	550	0.55	2000	475	8.2	7.4	1.12	L+FT
BA84-t0.55-S600	84	54	17	250	0.55	2500	600	5.8	5.1	1.15	L+FT
BA84-t0.55-S600	84	54	17	550	0.55	2500	600	5.9	5.2	1.15	L+FT
BA84-t0.55-S725	84	54	17	250	0.55	3000	725	4.3	3.6	1.22	L+FT
BA84-t0.55-S725	84	54	17	550	0.55	3000	725	4.9	4.1	1.20	L+FT
<b>BA-t0.7</b>											
BA84-t0.7-S75	84	54	17	250	0.70	250	75	29.1	25.1	1.16	L
BA84-t0.7-S75	84	54	17	550	0.70	250	75	42.2	37.9	1.11	L+F
BA84-t0.7-S175	84	54	17	250	0.70	625	175	28.7	24.2	1.18	L
BA84-t0.7-S175	84	54	17	550	0.70	625	175	34.3	33.8	1.01	L+FT
BA84-t0.7-S225	84	54	17	250	0.70	1000	225	27.2	22.8	1.19	L+FT
BA84-t0.7-S225	84	54	17	550	0.70	1000	225	31.8	30.4	1.04	L+FT
BA84-t0.7-S350	84	54	17	250	0.70	1500	350	17.7	15.2	1.17	L+FT
BA84-t0.7-S350	84	54	17	550	0.70	1500	350	19.8	18.1	1.09	L+FT
BA84-t0.7-S475	84	54	17	250	0.70	2000	475	11.3	10.3	1.10	L+FT
BA84-t0.7-S475	84	54	17	550	0.70	2000	475	12.3	12.5	0.99	L+FT
BA84-t0.7-S600	84	54	17	250	0.70	2500	600	8.2	8.4	0.97	L+FT
BA84-t0.7-S600	84	54	17	550	0.70	2500	600	8.3	8.7	0.96	L+FT
BA84-t0.7-S725	84	54	17	250	0.70	3000	725	6.5	6.1	1.07	L+FT
BA84-t0.7-S725	84	54	17	550	0.70	3000	725	6.6	6.4	1.03	L+FT
<b>BA-t0.85</b>											
BA84-t0.85-S75	84	54	17	250	0.85	250	75	41.0	35.8	1.15	L
BA84-t0.85-S75	84	54	17	550	0.85	250	75	56.6	52.3	1.08	L+F

Table 4 Continued

Specimen	First leg width	Second leg width	Lip depth	$F_y$	Thickness	Length	Screw spacing	FEA Results	Current DSM design strengths	Comparison	Failure modes
	$d_1$	$d_2$	$d_3$	-	$t$	$L$	-	$P_{FEA}$	$P_{DSM}$	$P_{FEA}/P_{DSM}$	-
	(mm)	(mm)	(mm)	MPa	(mm)	(mm)	(mm)	(kN)	(kN)	-	-
<b>BA-t0.85</b>											
BA84-t0.85-S175	84	54	17	250	0.85	625	175	40.2	34.6	1.16	L
BA84-t0.85-S175	84	54	17	550	0.85	625	175	53.9	50.2	1.07	L+FT
BA84-t0.85-S225	84	54	17	250	0.85	1000	225	36.7	31.7	1.16	L+FT
BA84-t0.85-S225	84	54	17	550	0.85	1000	225	48.5	41.1	1.18	L+FT
BA84-t0.85-S350	84	54	17	250	0.85	1500	350	22.3	20.8	1.07	L+FT
BA84-t0.85-S350	84	54	17	550	0.85	1500	350	22.6	20.9	1.08	L+FT
BA84-t0.85-S475	84	54	17	250	0.85	2000	475	14.4	12.5	1.15	L+FT
BA84-t0.85-S475	84	54	17	550	0.85	2000	475	16.1	15.1	1.07	L+FT
BA84-t0.85-S600	84	54	17	250	0.85	2500	600	10.1	8.6	1.17	L+FT
BA84-t0.85-S600	84	54	17	550	0.85	2500	600	12.2	12.4	0.98	L+FT
BA84-t0.85-S725	84	54	17	250	0.85	3000	725	7.3	6.4	1.14	L+FT
BA84-t0.85-S725	84	54	17	550	0.85	3000	725	10.0	9.8	1.03	L+FT
<b>BA-t3</b>											
BA84-t3-S75	84	54	17	250	3.00	250	75	215.9	226.5	0.95	L
BA84-t3-S75	84	54	17	550	3.00	250	75	443.6	477.3	0.93	L+F
BA84-t3-S175	84	54	17	250	3.00	625	175	185.5	194.0	0.96	L
BA84-t3-S175	84	54	17	550	3.00	625	175	317.1	322.9	0.98	L+FT
BA84-t3-S225	84	54	17	250	3.00	1000	225	154.8	155.6	0.99	L+FT
BA84-t3-S225	84	54	17	550	3.00	1000	225	200.0	194.9	1.03	L+FT
BA84-t3-S350	84	54	17	250	3.00	1500	350	121.9	115.9	1.05	L+FT
BA84-t3-S350	84	54	17	550	3.00	1500	350	141.0	125.2	1.13	L+FT
BA84-t3-S475	84	54	17	250	3.00	2000	475	99.7	95.7	1.04	L+FT
BA84-t3-S475	84	54	17	550	3.00	2000	475	107.1	98.4	1.09	L+FT
BA84-t3-S600	84	54	17	250	3.00	2500	600	81.7	83.4	0.98	L+FT
BA84-t3-S600	84	54	17	550	3.00	2500	600	84.0	84.2	1.00	L+FT
BA84-t3-S725	84	54	17	250	3.00	3000	725	70.9	73.5	0.96	L+FT
BA84-t3-S725	84	54	17	550	3.00	3000	725	71.9	73.4	0.98	L+FT
<b>BA-t5</b>											
BA84-t5-S75	84	54	17	250	5.00	250	75	348.5	354.0	0.98	L
BA84-t5-S75	84	54	17	550	5.00	250	75	734.3	742.0	0.99	L+F
BA84-t5-S175	84	54	17	250	5.00	625	175	306.9	314.0	0.98	L
BA84-t5-S175	84	54	17	550	5.00	625	175	547.4	574.3	0.95	L+FT
BA84-t5-S225	84	54	17	250	5.00	1000	225	284.7	290.5	0.98	L+FT
BA84-t5-S225	84	54	17	550	5.00	1000	225	456.4	442.1	1.03	L+FT
BA84-t5-S350	84	54	17	250	5.00	1500	350	257.4	264.6	0.97	L+FT
BA84-t5-S350	84	54	17	550	5.00	1500	350	336.0	356.0	0.94	L+FT
BA84-t5-S475	84	54	17	250	5.00	2000	475	209.1	214.6	0.97	L+FT
BA84-t5-S475	84	54	17	550	5.00	2000	475	249.8	258.5	0.97	L+FT
BA84-t5-S600	84	54	17	250	5.00	2500	600	148.8	163.2	0.91	L+FT
BA84-t5-S600	84	54	17	550	5.00	2500	600	175.7	171.1	1.03	L+FT
BA84-t5-S725	84	54	17	250	5.00	3000	725	121.0	117.9	1.03	L+FT
BA84-t5-S725	84	54	17	550	5.00	3000	725	132.2	121.0	1.09	L+FT
Mean										1.07	-
COV										0.08	-

\*L- Local buckling; FT- Flexural-torsional buckling; F-Flexural buckling

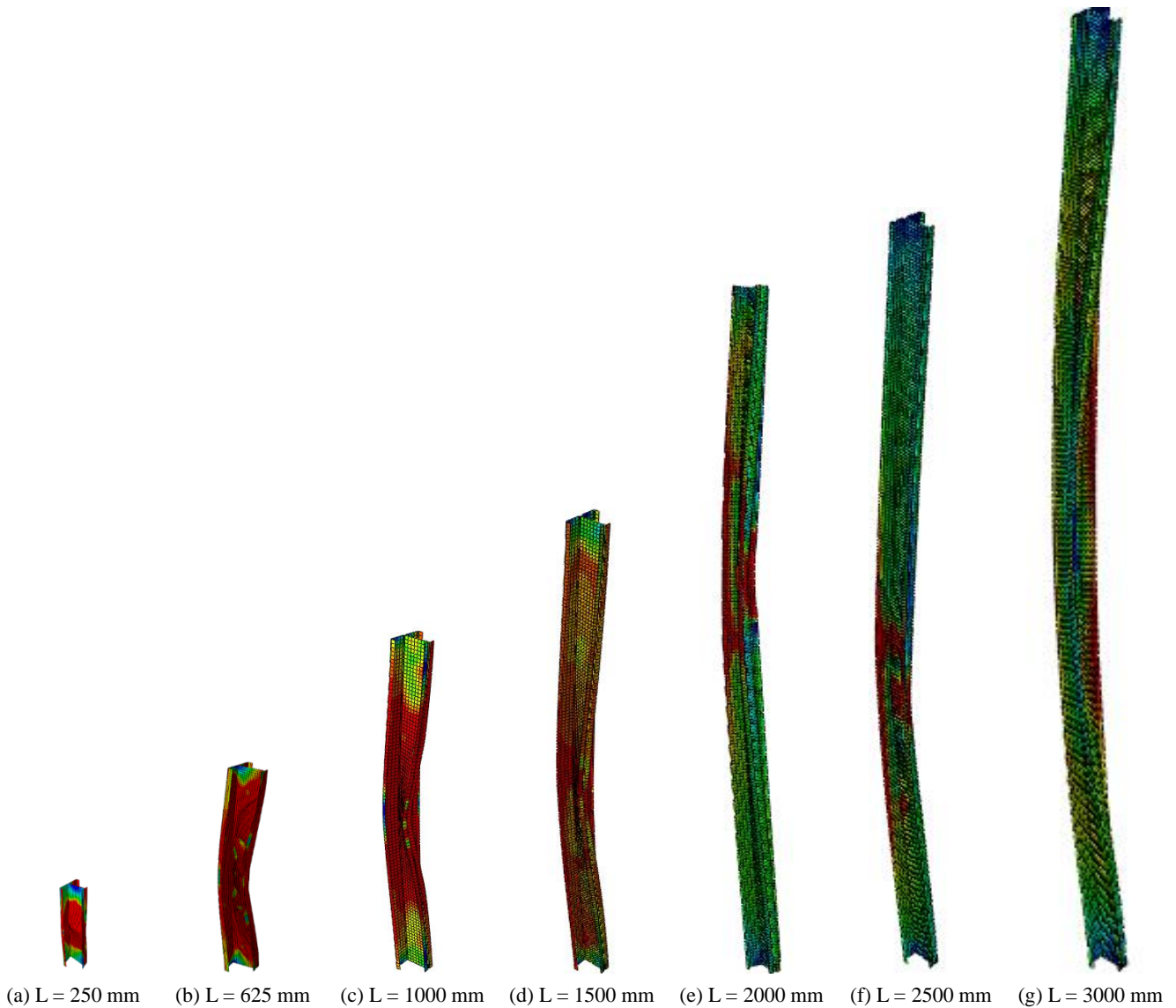


Fig. 15 Deformed shapes at failure for BA84-t3 series from the FEA for  $F_y = 250$  MPa

The nominal axial strength ( $P_{nd}$ ) for distortional buckling can be calculated using Eq. (11) as given below

$$P_{nd} = \begin{cases} P_y & \text{for } \lambda_d \leq 0.561 \\ \left[ 1 - 0.25 \left( \frac{P_{crd}}{P_y} \right)^{0.6} \right] \left( \frac{P_{crd}}{P_y} \right)^{0.6} P_y & \text{for } \lambda_d > 0.561 \end{cases} \quad (11)$$

Where  $\lambda_d = \sqrt{P_y / P_{crd}}$  and,  $P_{crd} = Af_{od}$ .

The above equations were used to calculate the design axial strength of back-to-back built-up CFS equal and unequal angle section columns, where the values of flexural ( $P_{ne}$ ), local ( $P_{nl}$ ), and distortional ( $P_{nd}$ ) buckling loads were calculated from the signature curves using the CUFSM (2018) software. The design axial strengths calculated using the DSM equations, were compared against the test and FE results for both the back-to-back built-up CFS unequal and equal angle section columns in Tables 2 and 4, respectively. The CUFSM (2018) software was also used to predict the possible buckling modes for back-to-

back built-up CFS unequal angle section columns under axial compression and the expected failure modes are shown in Fig. 14.

## 5. Parametric study

In order to verify the accuracy of the current design guidelines by Direct Strength Method (DSM), an extensive parametric study was conducted using the validated FE model for back-to-back built-up CFS unequal angle section column. The same cross-section of the unequal angle as tested (BA84), was used in the parametric study. Only screw-fastened connections were used to connect the back-to-back unequal angles in the parametric analysis. The parametric study was designed in such a way that five different thicknesses (0.55 mm, 0.7 mm, 0.85 mm, 3 mm and 5 mm), two different steel grades (250 MPa and 550 MPa) and seven different lengths (250 mm, 625 mm, 1000 mm, 1500 mm, 2000 mm, 2500 mm and 3000 mm) covering a wide range of slenderness from stub to slender

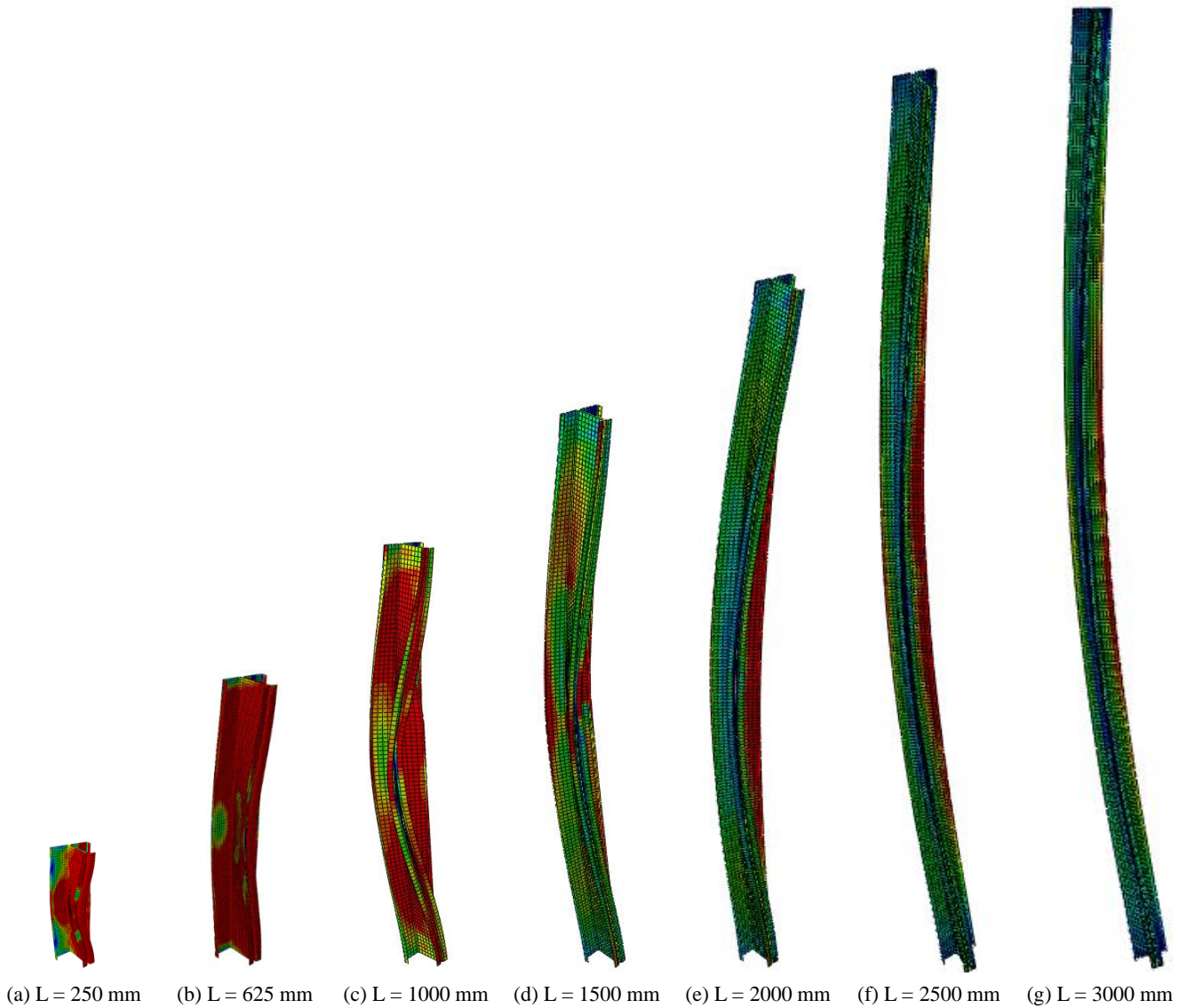


Fig. 16 Deformed shapes at failure for BA84-t5 series from the FEA for yield stress of 550 MPa

columns, was considered. In total, 70 FE models were analyzed.

The dimensions of the back-to-back built-up CFS unequal angle sections studied in the parametric analysis are shown in Table 4. As can be seen from Table 4, the built-up sections were labelled in such a way that the cross-sectional dimensions (BA84) of the unequal angles, their thickness (t) and the screw spacing (S) were defined by the label.

The axial strengths of the columns obtained from the FEA are also shown in Table 5. As can be seen from Table 4, significant strength reduction occurred for all columns beyond 1500 mm length irrespective of thickness. The failure modes of the back-to-back built-up CFS unequal angle section columns obtained from the FEA for BA84-t3 and BA84-t5 series for seven different lengths (250 mm, 625 mm, 1000 mm, 1500 mm, 2000 mm, 2500 mm and 3000 mm) are shown in Figs. 15 and 16 for yield stresses of 250 MPa and 550 MPa, respectively. As can be seen, clear flexural-torsional buckling was observed for columns higher than 1500 mm length. While, the stub columns

having lengths from 250 mm and 625 mm, failed by local buckling. Most of the intermediate (1000 mm, 1500 mm long) and slender (2000 mm, 2500 mm and 3000 mm long)

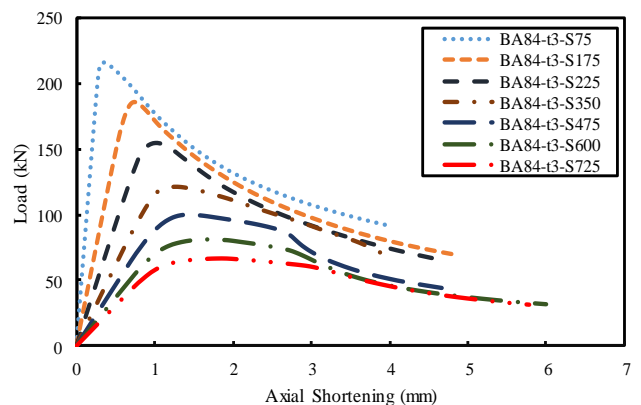


Fig. 17 Load versus axial shortening graphs for BA84-t3 series ( $F_y = 250$  MPa)

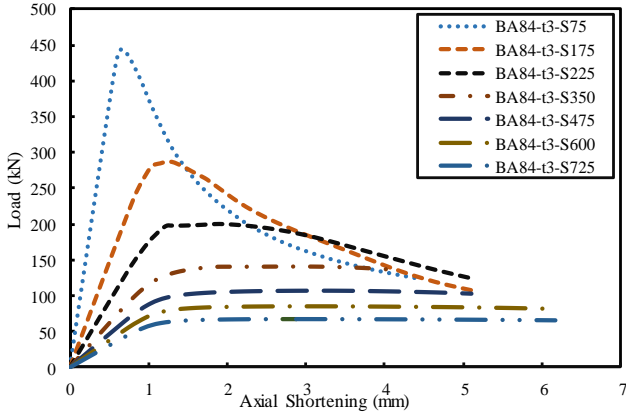


Fig. 18 Load versus axial shortening graphs for BA84-t3 series ( $F_y = 550$  MPa)

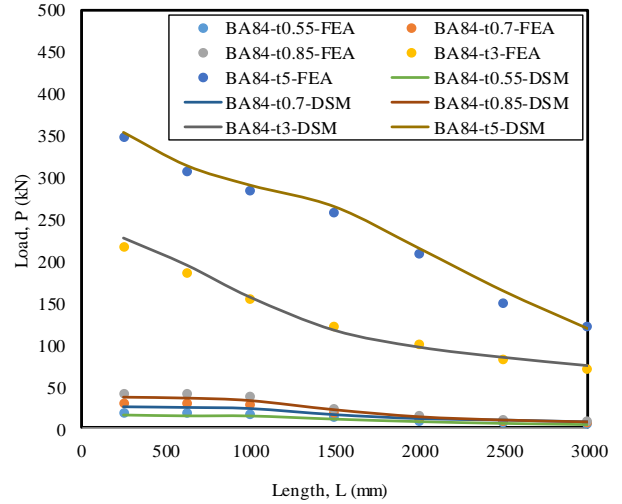


Fig. 19 Load versus length graphs ( $F_y = 250$  MPa)

columns failed at the mid-height irrespective of angle thickness.

Load-axial shortening curves for back-to-back built-up CFS unequal angle sections, covering stub to slender columns (250 mm to 3000 mm length) are shown in Figs. 17 and 18 for yield stresses of 250 MPa and 550 MPa, respectively. Figs. 19 and 20 plotted the relationship between the axial strength and length of the back-to-back built-up CFS unequal angle sections with yield stresses of 250 MPa and 550 MPa, respectively. As can be seen from

Figs. 19 and 20, there is a sudden decrease in load after 1500 mm length for higher thicknesses (3 mm and 5 mm). The current DSM was also used to calculate the design axial strength of the columns analyzed in the parametric study and the results are reported in Table 4. Figs. 21 and 22 show the relationship between the axial strengths calculated from calculated from the FEA ( $P_{FEA}$ ) and DSM ( $P_{DSM}$ ) for yield stressed of 250 MPa and 550 MPa, respectively. The results

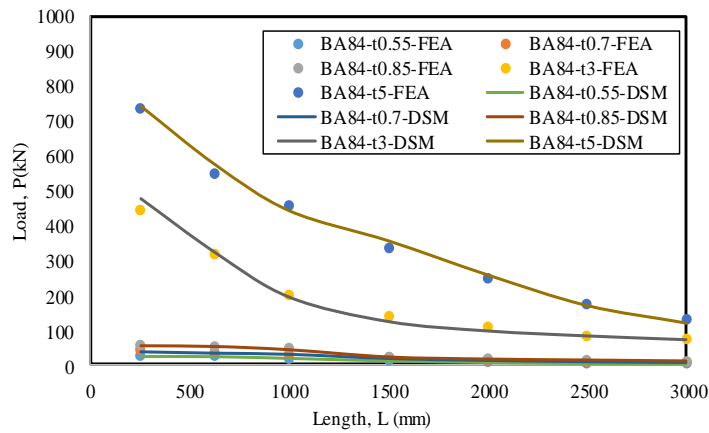


Fig. 20 Load versus length graphs ( $F_y = 550$  MPa)

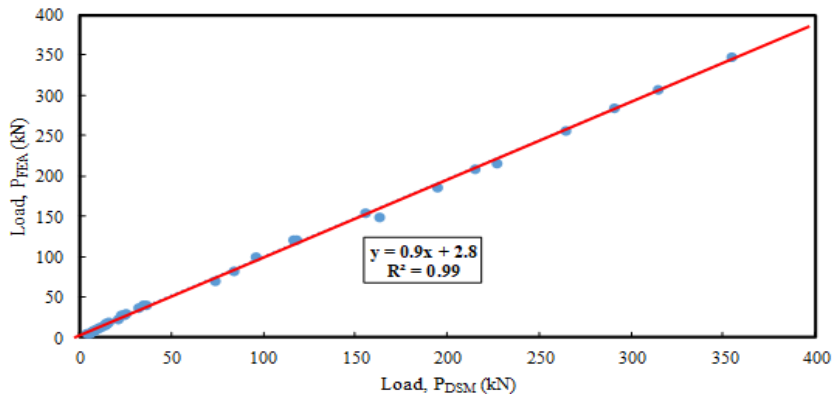


Fig. 21 Comparison of  $P_{FEA}$  versus  $P_{DSM}$  ( $F_y = 250$  MPa)

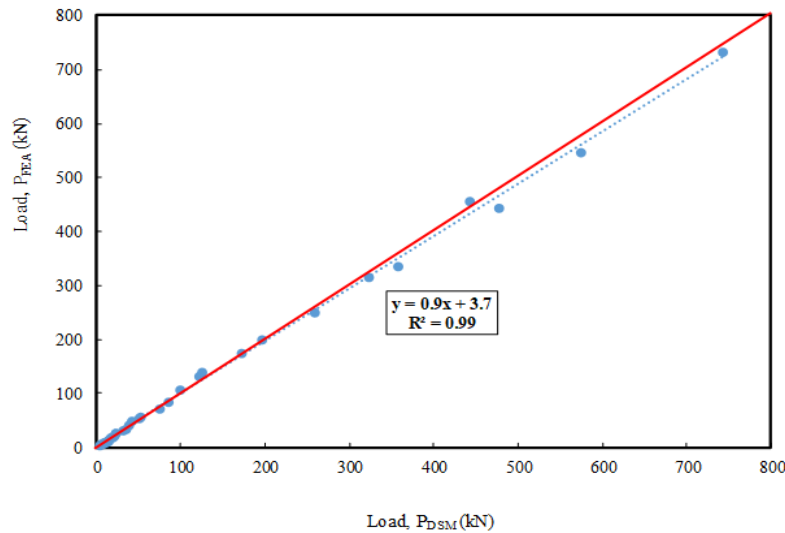


Fig. 22 Comparison of  $P_{FEA}$  versus  $P_{DSM}$  ( $F_y = 550$  MPa)

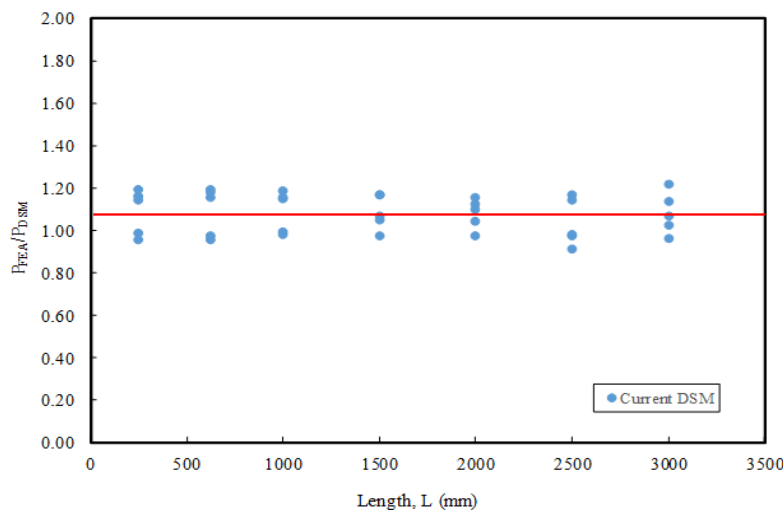


Fig. 23 Comparison of  $P_{FEA}$  and  $P_{DSM}$  results with varying length

obtained from the parametric study was used to achieve a good fit between the FEA and DSM results. For this purpose, a regression analysis was conducted for both the yield stresses and the obtained regression co-efficient was 0.99. Fig. 23 shows the variation of the ratio of FEA and DSM results ( $P_{FEA}/P_{DSM}$ ) with length of the built-up columns. It can be seen from Fig. 23 that the prediction of axial strength by FEA is higher than the DSM, irrespective of angle thickness.

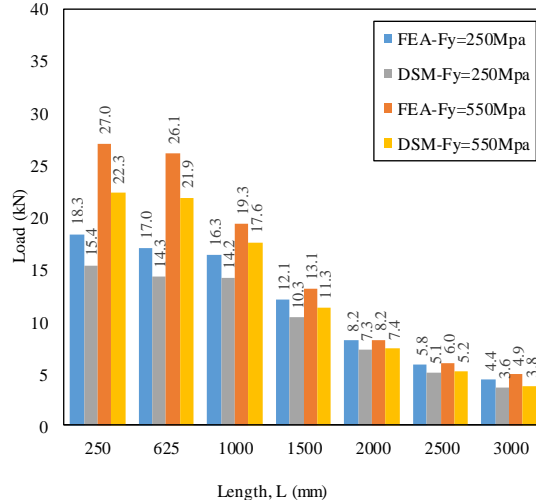
The axial strengths obtained from the FEA ( $P_{FEA}$ ) and DSM ( $P_{DSM}$ ) are plotted against the length of the built-up columns in Figs. 24(a), (b), (c), (d), and (e) for BA84-d17-t0.55, BA84-d17-t0.7, BA84-d17-t0.85, BA84-d17-t3 and BA84-d17-t5, respectively. Both the FEA and DSM results show a significant increase in the axial strengths when the yield stress was changed from 250 MPa to 550 MPa for 3 mm and 5 mm thick angles of stub and short columns. Similar behaviour was observed for intermediate and slender columns. From the comparison of FEA and DSM results (Table 4), it was found that the current design

guidelines by the DSM, can closely predict the axial strengths of back-to-back built-up CFS unequal angle section columns, being only 7% conservative to the test and FEA results.

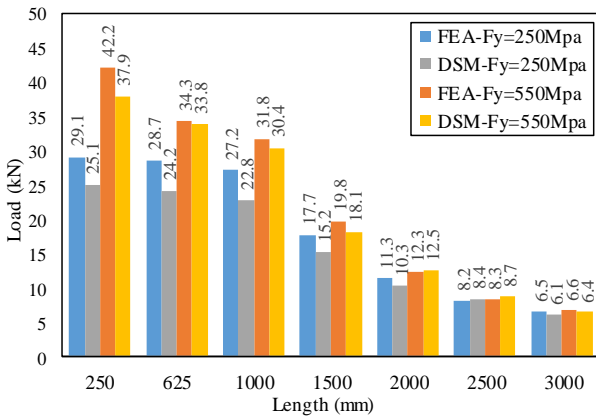
## 6. Conclusions

An experimental test program on axial strength of back-to-back built-up CFS unequal angle section columns is presented in this paper. Both the screw fastened, and welded connections were used to connect the unequal angle sections back-to-back, and the test results are reported. The failure modes, axial strengths, load-axial shortening and load-lateral displacement behaviour are discussed.

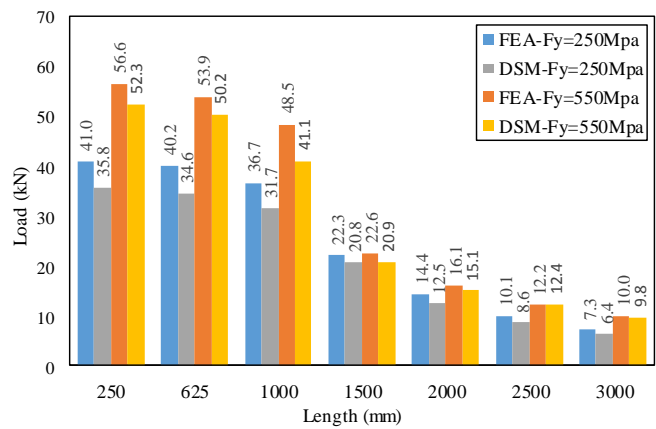
A nonlinear FE model was then developed for back-to-back built-up CFS unequal angle section column, which includes material non-linearity, geometric imperfections and modeling of intermediate fasteners. The FE model was validated against the experimental results of back-to-back



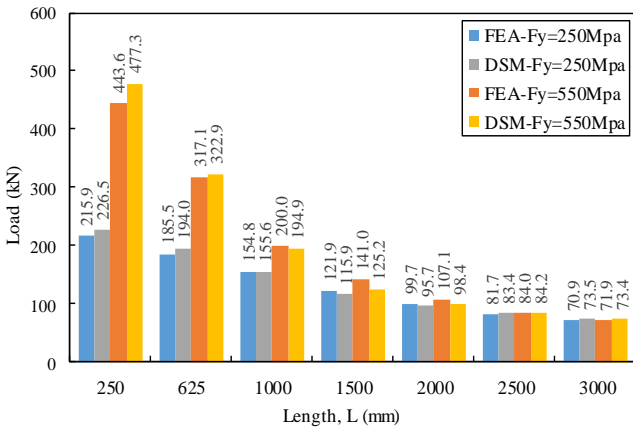
(a) BA84-t0.55 series



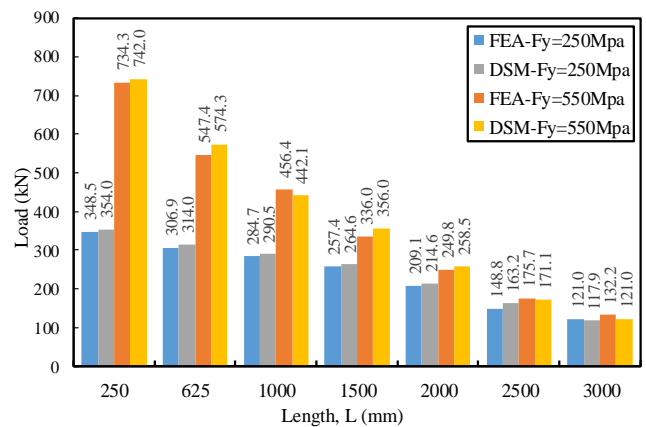
(b) BA84-t0.7 series



(c) BA84-t0.85 series



(d) BA84-t3 series



(e) BA84-t5 series

Fig. 24 Comparison of column strengths from the FEA and current DSM for back-to-back built-up unequal angle sections

built-up CFS unequal angle section columns, which showed good agreement both in terms of failure loads and deformed shapes. To check the reliability of the modelling technique, another FE model was developed and validated against the test results available in the literature for back-to-back built-up CFS equal angle section columns. From the comparison of FE and test results, it can be concluded that the FE models developed for both the back-to-back built-up CFS equal and unequal angle section columns, can be used to

predict the failure behavior of such built-up columns.

The validated FE model for back-to-back built-up CFS unequal angle section column was then used to perform a parametric study to investigate the effect of different thicknesses, lengths and, yield stresses of steel on axial strength of back-to-back built-up CFS unequal angle section columns. In total, 70 FE models were analyzed, covering a wide range of slenderness's from stub to slender columns. From the results of the parametric study, it was found that

the stub columns having lengths from 250 mm to 625 mm, failed by local buckling. As expected, the strength of the built-up columns decreased steadily with increase in length, irrespective of the yield stress. All the columns having lengths more than 625 mm, failed through a combination of local and flexural-torsional buckling.

The axial strengths predicted from the FEA were also compared against the design strengths calculated in accordance with the Direct Strength Method (DSM). The current DSM design rules underestimated the axial strength by 7% on average for back-to-back built-up CFS unequal angle section columns. The test results and the validated FE model can be used by the researchers and practicing engineers for predicting the axial strengths of back-to-back built-up CFS unequal angle section columns.

## References

- ABAQUS (2018), Version 6.14-2, SIMULIA, Providence, RI, USA.
- American Iron and Steel Institute (2016), North American specification for the design of cold-formed Steel Structural Members; NAS S100.
- Ananthi, G.B.G., Roy, K. and Lim, J.B.P. (2019), Experimental and numerical investigations on axial strength of back-to-back built-up cold-formed steel angle columns, *Steel Compos. Struct., Int. J.*, **31**(6), 601-615.  
<https://doi.org/10.12989/scs.2019.31.6.601>
- Anbarasu, M., Kanagarasu, K. and Sukumar, S. (2015), "Investigation on the behaviour and strength of cold-formed steel web stiffened built-up battened columns", *Mater. Struct.*, **48**(12), 4029-4038. <https://doi.org/10.1617/s11527-014-0463-8>
- ASTM: 370 - 92 (1996), Standard test methods and definitions for mechanical testing of steel products.
- CUFSM 5, 2018, Johns Hopkins University.
- Dabaon, M., Ellobody, E. and Ramzy, K. (2015), "Nonlinear behavior of built-up cold-formed steel section battened columns", *J. Constr. Steel Res.*, **110**, 16-28.  
<http://dx.doi.org/10.1016/j.engstruct.2005.07.005>
- Dar, M.A., Sahoo, D.R., Pulikkal, S. and Jain, A.K. (2018), "Behaviour of laced built-up cold-formed steel columns: Experimental investigation and numerical validation", *Thin-Wall. Struct.*, **132**, 398-409.  
<http://dx.doi.org/10.12989/scs.2018.27.5.545>
- EC3. Eurocode 3 (2005): Design of steel structures. Part 1-1: General rules and rules for building. British Standard Institution, BS EN 1993-1-1, London, UK.
- Ellobody, E. and Young, B. (2007), "Design of cold-formed steel unequal angle compression members", *J. Constr. Steel Res.*, **45**, 330-338.  
<https://doi.org/10.1016/j.tws.2007.02.015>
- Fratamico, D.C., Torabian, S., Rasmussen, K.J. and Schafer, B.W. (2016), "Experimental investigation of the effect of screw fastener spacing on the local and distortional buckling behavior of built-up cold-formed steel columns", *Proceedings of 'Wei-Wen Yu International Specialty Conference on Cold-Formed Steel Structures 2018'*, Baltimore, MD, USA, November.
- Georgieva, I., Schueremans, L. and Lincy, P. (2012), "Composed columns from cold-formed steel Z-profiles: experiments and code based predictions of the overall compression capacity", *Eng. Struct.*, **37**, 125-134.  
<https://doi.org/10.1016/j.engstruct.2011.12.017>
- Kyvelou, P., Gardner, L. and Nethercot, D.A. (2017), "Design of composite cold-formed steel flooring systems", *Struct.*, **12**, 242-252. <https://doi.org/10.1016/j.istruc.2017.09.006>
- Lim, J.B.P. and Nethercot, D.A. (2003), "Serviceability design of a cold-formed steel portal frame having semi-rigid joints", *Steel Compos. Struct., Int. J.*, **3**(6), 451-474.  
<https://doi.org/10.12989/scs.2003.3.6.451>
- Lian, Y., Uzzaman, A., Lim, J.B.P., Abdelal, G., Nash, D. and Young, B. (2017), "Web crippling behaviour of cold-formed steel channel sections with web holes subjected to interior-one-flange loading condition - Part II: parametric study and proposed design equations", *Thin-Wall. Struct.*, **114**, 92-106.  
<http://dx.doi.org/10.1016/j.tws.2016.10.018>
- Lu, Y., Zhou, T., Li, W. and Wu, H. (2017), "Experimental investigation and a novel direct strength method for cold-formed built-up I-section columns", *Thin-Wall. Struct.*, **112**, 125-139.  
<https://doi.org/10.1016/j.tws.2016.12.011>
- Piyawat, K., Ramseyer, C. and Kang, T.H.K. (2013), "Development of an axial load capacity equation for doubly symmetric built-up cold-formed sections", *J. Struct. Eng. Am. Soc. Civil Engr.*, **139**(12), 04013008-04013013.  
[https://doi.org/10.1061/\(ASCE\)ST.1943-541X.0000780](https://doi.org/10.1061/(ASCE)ST.1943-541X.0000780)
- Reyes, W. and Guzmán, A. (2011), "Evaluation of the slenderness ratio in built-up cold-formed box sections", *J. Constr. Steel Res.*, **67**, 929-935. <https://doi.org/10.1016/j.jcsr.2011.02.003>
- Roy, K., Ting, T.C.H., Lau, H.H. and Lim, J.B.P. (2018a), "Effect of thickness on the behaviour of axially loaded back-to-back cold-formed steel built-up channel sections - Experimental and numerical investigation", *Struct.*, **16**, 327-346.  
<https://doi.org/10.1016/j.istruc.2018.09.009>
- Roy, K., Ting, T.C.H., Lau, H.H. and Lim, J.B.P. (2018b), "Nonlinear behaviour of back-to-back gapped built-up cold-formed steel channel sections under compression", *J. Constr. Steel Res.*, **147**, 257-276.  
<https://doi.org/10.1016/j.jcsr.2018.04.007>
- Roy, K., Ting, T.C.H., Lau, H.H. and Lim, J.B.P. (2018c), "Nonlinear behavior of axially loaded back-to-back built-up cold-formed steel un-lipped channel sections", *Steel Compos. Struct., Int. J.*, **28**(2), 233-250.  
<https://doi.org/10.12989/scs.2018.28.2.233>
- Roy, K., Ting, T.C.H., Lau, H.H. and Lim, J.B.P. (2018d), "Effect of screw spacing on behavior of axially loaded back-to-back cold-formed steel built-up channel sections", *Adv. Struct. Eng.*, **21**(3), 474-487.  
<https://doi.org/10.1177/1369433217719986>
- Roy, K., Mohammadjani, C. and Lim, J.B.P. (2019a), "Experimental and numerical investigation into the behaviour of face-to-face built-up cold-formed steel channel sections under compression", *Thin-Wall. Struct.*, **134**, 291-309.  
<https://doi.org/10.1016/j.tws.2018.09.045>
- Roy, K., Ting, T.C.H., Lau, H.H. and Lim, J.B.P. (2019b), "Experimental and numerical investigations on the axial capacity of cold-formed steel built-up box sections", *J. Constr. Steel Res.*, **160**, 411-427.  
<https://doi.org/10.1016/j.jcsr.2019.05.038>
- Schafer, B.W. and Pekoz, T. (1998), "Computational modelling of cold-formed steel: characterizing Geometric imperfections and residual stress", *J. Constr. Steel Res.*, **47**, 193-210.  
[https://doi.org/10.1016/S0143-974X\(98\)00007-8](https://doi.org/10.1016/S0143-974X(98)00007-8)
- Shi, G., Liu, Z., Ban, H.Y., Zhang, Y., Shi, Y.J. and Wang, Y.Q. (2011), "Tests and finite element analysis on the local buckling of 420 MPa steel equal angle columns under axial compression" *Steel Compos. Struct., Int. J.*, **12**(1), 31-51.  
<https://doi.org/10.12989/scs.2011.12.1.031>
- Standards Australia (2018), Cold-Formed Steel Structures, AS/NZS 4600:2018, Standards Australia/ Standards New Zealand.
- Stone, T.A. and LaBoube, R.A. (2005), "Behaviour of cold-formed steel built-up I-sections", *Thin-Wall. Struct.*, **43**(12), 1805-1817.

- <https://doi.org/10.1016/j.tws.2005.09.001>
- Ting, T.C.H., Roy, K., Lau, H.H. and Lim, J.B.P. (2018), "Effect of screw spacing on behavior of axially loaded back-to-back cold-formed steel built-up channel sections", *Adv. Struct. Eng.*, **21**(3), 474-487. <https://doi.org/10.1177/1369433217719986>
- Uzzaman, A., Lim, J.B., Nash, D., Rhodes, J. and Young, B. (2012a), "Cold-formed steel sections with web openings subjected to web crippling under two-flange loading conditions—part I: Tests and finite element analysis", *Thin-Wall. Struct.*, **56**, 38-48. <https://doi.org/10.1016/j.tws.2012.03.010>
- Uzzaman, A., Lim, J.B., Nash, D., Rhodes, J. and Young, B. (2012b), "Cold-formed steel sections with web openings subjected to web crippling under two-flange loading conditions—Part II: Parametric study and proposed design equations", *Thin-Wall. Struct.*, **56**, 79-87. <https://doi.org/10.1016/j.tws.2012.03.009>
- Uzzaman, A., Lim, J.B.P., Nash, D. and Young, B. (2017), "Effects of edge-stiffened circular holes on the web crippling strength of cold-formed steel channel sections under one-flange loading conditions", *Eng. Struct.*, **139**, 96-107. <http://dx.doi.org/10.1016/j.engstruct.2017.02.042>
- Vishnuvardhan, S. (2006), "Behaviour of cold-formed steel single and compound angles in compression", Ph.D. Dissertation; Anna University, Chennai, India.
- Whittle, J. and Ramseyer, C. (2009), "Buckling capacities of axially loaded, cold-formed, built-up channels", *Thin-Wall. Struct.*, **47**(2), 190-201. <https://doi.org/10.1016/j.tws.2008.05.014>
- Ye, J., Hajirasouliha, I. and Becque, J. (2018a), "Experimental investigation of local-flexural interactive buckling of cold-formed steel channel columns", *Thin-Wall. Struct.*, **125**, 245-258. <https://doi.org/10.1016/j.tws.2018.01.020>
- Ye, J., Mojtabaie, S.M. and Hajirasouliha, I. (2018b), "Local-flexural interactive buckling of standard and optimised cold-formed steel columns", *J. Constr. Steel Res.*, **144**, 106-118. <https://doi.org/10.1016/j.jcsr.2018.01.012>
- Young, B. and Chen, J. (2008), "Column tests of cold-formed steel non-symmetric lipped angle sections", *J. Constr. Steel Res.*, **64**, 808-815. <https://doi.org/10.1016/j.jcsr.2008.01.021>
- Zhang, J.H., Young, B. (2012), "Compression tests of cold-formed steel I-shaped open sections with edge and web stiffeners", *Thin-Wall. Struct.*, **52**, 1-11. <https://doi.org/10.1016/j.tws.2011.11.006>

## Notations

A	Gross area of the section;
AISI	American Iron and Steel Institute;
AS/NZS	Australian and New Zealand Standards;
CFS	Cold-formed steel;
COV	Coefficient of variation;
$d_1$	First leg width of the angle section;
$d_2$	Second leg width of the angle section;
$d_3$	Overall lip depth of the angle section;
DSM	Direct Strength Method;
$E$	Modulus of elasticity;
EWM	Effective Width Method;
$F_y$	Yield strength;
$F_u$	Ultimate tensile strength of steel;
FEM	Finite element modelling;
$f_{od}$	Distortional buckling stress;
$f_{ol}$	Elastic local buckling stress;
$f_y$	Yield stress;
K	Effective length factor;
L	Unbraced member length;
$L_o$	Gauge Length;
$P_{cre}$	Critical elastic flexural buckling load;
$P_{FEA}$	Axial strength from experiments;
$P_{EXP}$	Axial strength from the finite element analysis;
$P_{DSM}$	Axial strength calculated by Direct Strength Method;
$P_{ne}$	Nominal axial strength for flexural buckling;
$P_{nd}$	Nominal axial strength for distortional buckling;
$P_{nl}$	Nominal axial strength for local buckling;
S	Screw spacing;
t	Thickness;
T	Base metal thickness;
$\lambda$	Slenderness ratio;